JACS
JOURNAL OF THE AMERICAN CHEMICAL SOCIETY

COMMUNICATION

pubs.acs.org/JACS

Interrupted Zeolite LTA and ATN-Type Boron Imidazolate Frameworks

Hai-Xia Zhang,[†] Fei Wang,[†] Hui Yang,[†] Yan-Xi Tan,[†] Jian Zhang,*[,†] and Xianhui Bu*[,‡]

[†]State Key Laboratory of Structural Chemistry, Fujian Institute of Research on the Structure of Matter, Chinese Academy of Sciences, Fuzhou, Fujian 350002, P. R. China

[‡]Department of Chemistry and Biochemistry, California State University, Long Beach, 1250 Bellflower Boulevard, Long Beach, California 90840, United States

Supporting Information

ABSTRACT: Zeolite A (LTA) is of much interest in zeolite family because of its large-scale industrial applications. Making Zeolite A (a typical 4-connected tetrahedral framework material) with a lower connectivity (3-connected) might lead to new open architecture with expanded ring size and enhanced functionality. The first interrupted Zeolite A with 3-connected network has been experimentally realized here by a boron imidazolate (im) framework material (BIF-20) with 3-coordinate $BH(mim)_3^-$ building units. Additionally, a new strategy toward the construction of functional microporous metal−organic frameworks with interrupted zeolite-type topologies is presented by both 3-connected boron imidazolate frameworks (BIF-20 and BIF-21). BIF-20 has an unusual tetrahedral framework with both debonded α and β cages, and exhibits high H_2 uptake capacity.

Search for functional porous materials continues to attract much attention in some currently emerging areas related to health, energy use, and environmental conservation.[1−4] A currently very active area is to make zeolite-type metal−organic frameworks (MOFs) due to their potential applications in catalysis, gas storage, and separation.[5−8] The early synthetic efforts focused on the use of divalent metal cations (Zn^{2+} in particular) and imidazolate ligands (im) with different substituents to replace Si^{4+} (Al^{3+}) and O^{2-} in zeolites, respectively, resulting in a series of zeolitic imidazolate frameworks (ZIFs) with high chemical and thermal stability.[6] ZIFs have tunable zeolite-type topologies (e.g., SOD, RHO, LTA, etc.) and promising applications for the capture of CO_2.[6e] We are particularly interested in searching new compositional domains for metal organic zeolites. Our success is based on the cross-linking of various presynthesized boron imidazolate complexes by tetrahedral cations (e.g., Li^+ and Cu^+) into extended lightweight boron imidazolate frameworks (BIFs).[8]

Most of zeolites with TO_4 units and ZIFs with $Zn(im)_4$ units are typical four-connected networks in which tetrahedral centers are fully surrounded by the μ_2-linkers.[4] Only several interrupted zeolite frameworks (e.g,, -CLO, JDF-20) with hydroxide groups and ZIF-100 are known to contain 3-connected nodes in the zeolite-type topologies.[9,6d] Theoretically, removing one linker from each tetrahedral node should make interrupted zeolites and ZIFs with opened rings and 3-coordinate centers (Figure 1a,b). Furthermore, the 3-coordinate centers might have modifiable (or coordinatively unsaturated) sites which have been shown to be desirable for enhancing gas uptake capacity and for promoting catalytic activity.[2] However, the controllable generation of TO_3 or $Zn(im)_3$ unit still remains a synthetic challenge. Some early examples of framework materials with 3-connected centers are based on metal methylphosphonates ($CH_3PO_3^{2-}$).[10a,b] Later efforts on metal phosphites (HPO_3^{2-}) have been shown to have limited success for fabricating porous 3-connected zeolitic frameworks.[10c] Fortunately, BIFs present a great opportunity because both 4-connected $B(im)_4^-$ and 3-connected $BH(im)_3^-$ can be readily synthesized prior to the solvothermal assembly.[8a] The unique features of $BH(im)_3^-$ ligand include its 3-coordinate nature of the tetrahedral B center and the presence of the potentially active or functionalizable B−H bond (Figure 1c).

In this work, we apply such new strategy toward the construction of 3-connected zeolitic framework materials by employing the $BH(mim)_3^-$ (mim = 2-methyl-imidazolate) ligand. An interrupted zeolite A (LTA) framework $Zn_2(BH(mim)_3)_2$(obb) (**BIF-20**, obb = 4,4′-oxybis(benzoate)) and another interrupted ATN-type framework $Zn_2(BH(mim)_3)_2$(bpdc) (**BIF-21**, H_2bpdc = diphenic acid) were successfully synthesized and structurally charaterized.[11,12] Interestingly, **BIF-20** has an unusual 3-connected tetrahedral framework with both debonded α and β cages, and exhibits high H_2 uptake capacity.

Zeolite A (LTA) which has both α and β cages in the structure is of much interest in zeolite family, and the first reported LTA-type metal organic frameworks are ZIF-20 and ZIF-21 with purinate as the linkers. Until now, no other MOFs or ZIFs with LTA topology are known. **BIF-20** represents an unusual interrupted LTA network because of its 3-connected nature between two kinds of tetrahedral centers (Zn and B), in which the forth site of each tetrahedral Zn^{2+} center is just coordinated by a mononegatively charged carboxylate (COO^-) group (Figure 1c). The Zn−B connectivity in **BIF-20** features a previously unknown 3-connected net with vertex symbol of $(6.8.10)(6.8^2)(8^2.10)(8^3)$ (denoted: **fjz**) which is derived from the well-known LTA topology by omitting one linker from each tetrahedral node.[13] After removing one-quarter of linkers, all 4-rings in the LTA net are opened, leading to the generation of six 8-rings in each β-cage and six 12-rings in each α-cage (Figure 1a,b).

The synthesis of **BIF-20** was performed by mixing $KBH(mim)_3$, $Zn(NO_3)_2 \cdot 6(H_2O)$, and H_2obb in 2-amino-1-butanol/CH_3CN/*N*,*N*′-dimethylformamide (DMF) solvent at 80 °C for 4 days. The structure is fully characterized by single-crystal X-ray diffraction. The crystals of **BIF-20** are stable in air and insoluble in common solvents, such as water, methanol, and DMF.

Received: May 3, 2011
Published: July 15, 2011

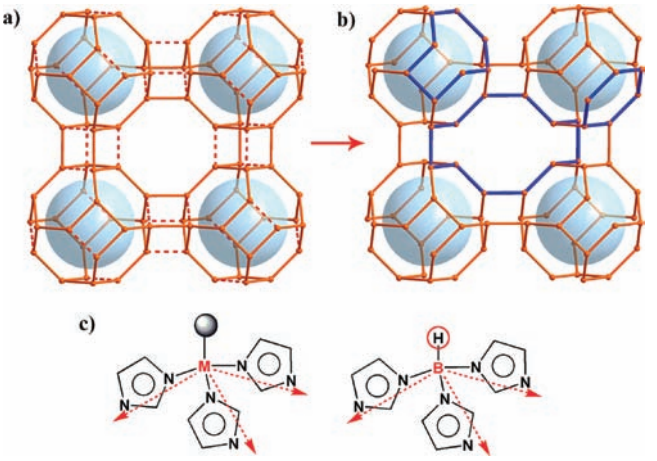

Figure 1. The design strategy for interrupted zeolite A. (a) LTA net; (b) interrupted LTA net (**fjz** net); (c) the building units for the construction of 3-connected zeolitic framework.

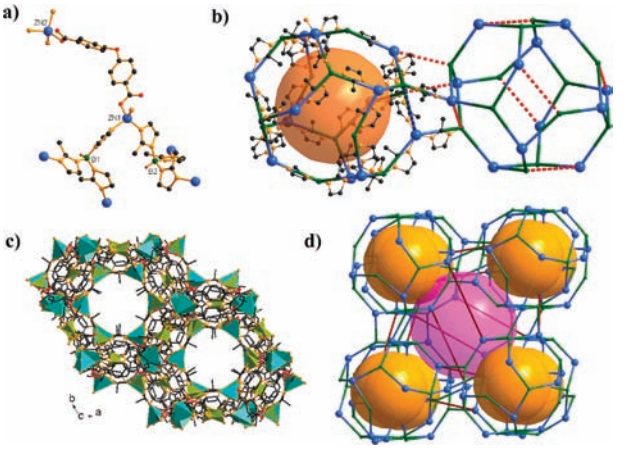

Figure 2. The structure and topology of **BIF-20**. (a) The coordination environment in **BIF-20**. (b) Two debonded β-cages where the red dashed lines indicate the interrupted Zn−B bonds. (c) The 3D framework with 1D channels. (d) The topological net of **BIF-20** where the red bonds represent the obb ligands.

BIF-20 has a neutral framework with tetrahedrally coordinated Zn and B nodes, but each Zn node is only bound by three tridentate $BH(mim)_3$ ligands and its forth coordination site is covered by the carboxylate oxygen atom from the bridging obb ligand (Figure 2a). The alternating linkage between tetrahedral Zn and B nodes via mim results in the formation of a 3-connected net with large cages (Figure 2b−d). The ideal topology for this net is **fjz** mentioned above, an interrupted LTA. However, the framework of **BIF-20** is much distorted due to the unequal bond lengths around Zn and B. Twelve $BH(mim)_3$ ligands use 30 mim linkers to join 12 Zn nodes, generating a debonded β-cage. Meanwhile, the remaining six mim linkers further connect six debonded β-cages from six directions, resulting in cubic packing of the cages and generation of a debonded α-cage (Figure 2d). The pore sizes of such two different cages are 12.0 and 16.0 Å in diameter, respectively, which are a little larger than those in the LTA-type ZIF-20.[6b] It is noteworthy that the pore space of the α-cage in **BIF-20** is partitioned by the obb ligands into several small spaces (Figure 2d). The presence of the obb ligands in **BIF-20** is also important because they serve as the charge balancing agents and the struts between the β-cages. **BIF-20** also shows 1D channels along the *c* axis, and the effective hexagonal window size of the channel is about 3.1 Å (Figure 2c). The density (T/V) expressed as the number of cationic nodes per unit volume is 2.55 nm^{-3}, larger than that of ZIF-20 (2.04 nm^{-3}).

BIF-20 contains structurally disordered solvent molecules in the pores (about 11 wt %) which can be exchanged by ethanol, as evidenced by the thermal gravimetric analysis (TGA, see Supporting Information). Further powder X-ray diffraction investigation indicated that the host framework of **BIF-20** is stable up to 350 °C without any change. The ethanol-exchanged and activated samples were used for gas sorption measurements.

Small windows and yet large inner cages in **BIF-20** led to unusual gas sorption behavior. The permanent porosity of desolvated **BIF-20** was established by N_2 sorption experiments at 77 K, which showed type I adsorption isotherm behavior and unusual hysteresis upon desorption (Figure 3a). This could be due to hindered diffusion through the narrow pore apertures. The calculated Langmuir and BET surface areas were 306 and 229 m^2/g, respectively. A single data point at relative pressure of 0.011 gives a maximum pore volume of 0.083 cm^3/g by the Horvath−Kawazoe equation. Such low N_2 uptake may be due to the small window size in **BIF-20** compared to the dynamic diameter of N_2 (0.36 nm). Similar behavior was also observed in ZIF-11.[6a]

The adsorption isotherms of CO_2 for **BIF-20** were measured up to 1 bar at 273 and 298 K, respectively (Figure 3b). The CO_2 uptake values are 53.9 cm^3/g (2.41 mmol/g) at 273 K and 34.8 cm^3/g (1.55 mmol/g) at 298 K, which are comparable to some highly porous ZIFs (e.g., ZIF-8, ZIF-100).[6e] The property of **BIF-20** related to the CO_2/N_2 separation under ambient conditions has also been investigated. The adsorption isotherms of N_2 for **BIF-20** were measured up to 1 bar at 273 and 298 K, respectively. However, N_2 was hardly adsorbed at all (only 9.5 cm^3/g at 273 K and 1.9 cm^3/g at 298 K) (Figure 3a).

Remarkably, the initial hydrogen uptake of **BIF-20** at 77 K and 1 atm is 1.43 wt % (Figure 3c), which is almost equal to that of ZIF-11 and significantly higher than that of LTA-type ZIF-20 (1.1 wt %). As a further test, a second H_2 adsorption isotherm was measured at 87 K, and two data sets were used to determine the isosteric heat of H_2 adsorption (Q_{st}). The initial Q_{st} value is estimated to be 6.1 kJ mol^{-1}, which is moderate compared with the other porous materials.

To demonstrate the general applicability of this approach for the construction of interrupted zeolite-type frameworks, another interrupted ATN-type framework material $Zn_2(BH(mim)_3)_2(bpdc)$ (**BIF-21**) was obtained by replacing the auxiliary obb ligand in **BIF-20** with the bpdc ligand. As proposed before, the structural topology of ZIF is mainly determined by link−link interactions, whereas for zeolite, it is controlled by the structure directing agents.[4,6] For **BIF-20** and **BIF-21**, their distinct topologies are based on the use of different charge balancing auxiliary ligands.

Figure 4 shows the detailed structural feature of **BIF-21**. Similar to **BIF-20**, each tetrahedral Zn node is coordinated by three tridentate $BH(mim)_3$ ligands and one carboxylate oxygen atom from the bridging bptc ligand (Figure 4c). However, the $BH(mim)_3$ ligands connect the Zn nodes into a 3-connected open framework with topology of **lig** (vertex symbol: $8.8.10_3$) (Figure 4b-d). Actually, the 3-connected **lig** net is closely related with the zeolite ATN topology, and can be derived from it when all 4-rings in ATN net are broken by losing one linker (Figure 4a-b). Thus, the **lig** net is an interrupted ATN net with larger

dx.doi.org/10.1021/ja2040927 |*J. Am. Chem. Soc.* 2011, 133, 11884–11887

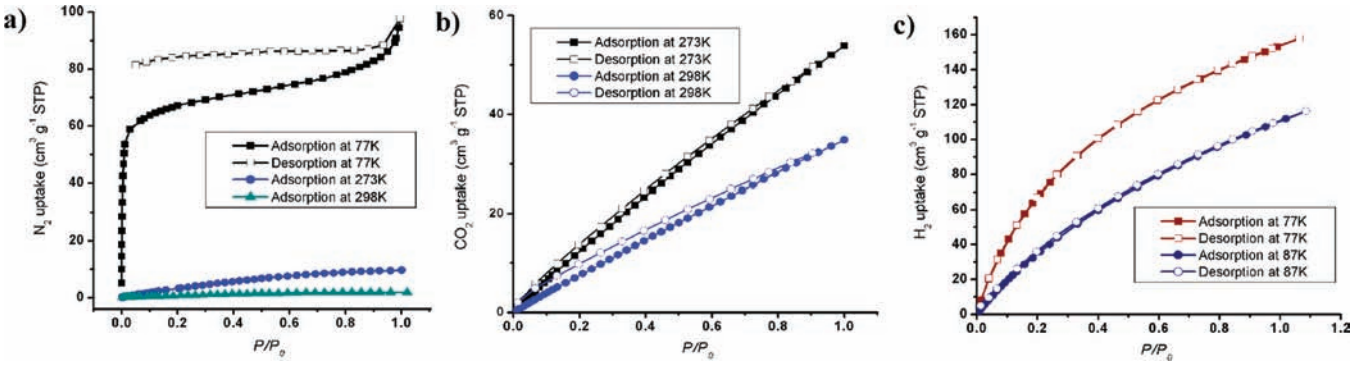

Figure 3. The gas sorption isotherms of **BIF-20**. P/P_0 is the ratio of gas pressure (P) to saturation pressure (P_0), with P_0 = 760 mmHg. (a) N_2; (b) CO_2; (c) H_2.

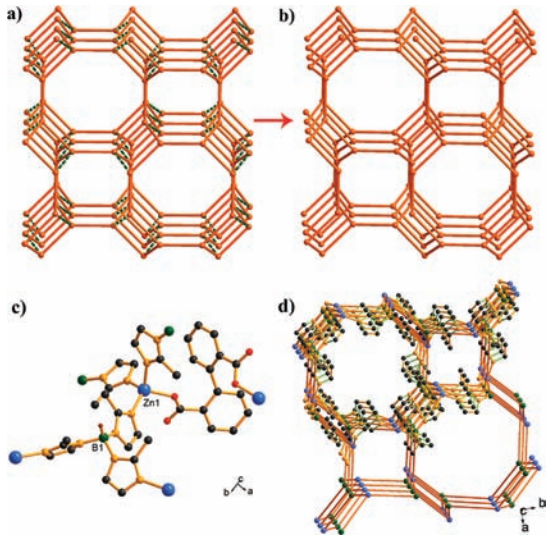

Figure 4. The structure and topology of **BIF-21**. (a) The 4-connected ATN net. (b) The 3-connected **lig** net. (c) The coordination environment in **BIF-21**. (d) The topological net of **BIF-21**.

10-rings. Two kinds of channels along the *c* axis are observed in **BIF-21**. The small channels are blocked by the bpdc ligands, while the large channels with dimension of 5.2 × 5.2 Å^2 are filled by the disordered solvent molecules. The framework density (T/V) is 2.80 nm^{-3}, which is larger than that of **BIF-20**.

In summary, we developed here a new strategy for the design of interrupted zeolite-type metal organic frameworks. Through the assembly of the $BH(mim)_3$ unit with the tetrahedral metal center, mediated with charge balancing carboxylate ligand, two interrupted zeolite LTA and ATN topologies were successfully realized by two BIF materials. The results revealed that the structural diversity of these materials could be easily tuned via adjusting both the imidazolate link and the auxiliary charge balancing carboxylate ligand. This work opened a new route toward the construction of novel zeolite-type framework materials.

■ ASSOCIATED CONTENT

Ⓢ Supporting Information. TGA diagram, powder X-ray diffraction, IR spectra and CIF files. This material is available free of charge via the Internet at http://pubs.acs.org.

■ AUTHOR INFORMATION

Corresponding Author
zhj@fjirsm.ac.cn; xbu@csulb.edu

■ ACKNOWLEDGMENT

We thank the support of this work by 973 program (2011CB932504), NSFC (21073191), the Innovation Program of CAS (KJCX2-YW-H21), and NSF (X.B., DMR-0846958).

■ REFERENCES

(1) (a) Férey, G. *Chem. Soc. Rev.* **2008**, *37*, 191. (b) Cheetham, A. K.; Férey, G.; Loiseau, T. *Angew. Chem., Int. Ed.* **1999**, *38*, 3268.

(2) (a) Long, J. R.; Yaghi, O. M. *Chem. Soc. Rev.* **2009**, *38*, 1213. (b) Ma, L.; Abney, C.; Lin, W. *Chem Soc. Rev.* **2009**, *38*, 1248. (c) Lee, J. Y.; Farha, O. K.; Roberts, J.; Scheidt, K. A.; Nguyen, S. T.; Hupp, J. T. *Chem. Soc. Rev.* **2009**, *38*, 1450. (d) Horike, S.; Shimomura, S.; Kitagawa, S. *Nat. Chem.* **2009**, *1*, 695.

(3) (a) Morris, R. E.; Wheatley, P. S. *Angew. Chem., Int. Ed.* **2008**, *47*, 4966. (b) Ma, S.; Zhou, H. *Chem. Commun.* **2010**, *46*, 44. (c) Yang, S.; Lin, X.; Blake, A. J.; Walker, G.; Hubberstey, P.; Champness, N. R.; Schröder, M. *Nat. Chem.* **2009**, *1*, 487.

(4) (a) Cooper, E. R.; Andrews, C. D.; Wheatley, P. S.; Webb, P. B.; Wormald, P.; Morris, R. E. *Nature* **2004**, *430*, 1012. (b) Bu, X. H.; Feng, P. Y.; Stucky, G. D. *Science* **1997**, *278*, 2080. (c) Van Bekkum, H.; Flanigen, E. M.; Jacobs, P. A; Jansen, J. C. *Introduction to Zeolite Science and Practice*; Elsevier: Amsterdam, 2001.

(5) (a) Tian, Y. Q.; Cai, C. X.; Ji, Y.; You, X. Z.; Peng, S. M.; Lee, G. S. *Angew. Chem., Int. Ed.* **2002**, *41*, 1384. (b) Tian, Y.-Q.; Zhao, Y.-M.; Chen, Z.-X.; Zhang, G.-N.; Weng, L.-H.; Zhao, D.-Y. *Chem.—Eur. J.* **2007**, *13*, 4146. (c) Huang, X.-C.; Lin, Y.-Y.; Zhang, J. P.; Chen, X.-M. *Angew. Chem., Int. Ed.* **2006**, *45*, 1557. (d) Nouar, F.; Eckert, J.; Eubank, J. F.; Forster, P.; Eddaoudi, M. *J. Am. Chem. Soc.* **2009**, *131*, 2864.

(6) (a) Park, K. S.; et al. *Proc. Natl. Acad. Sci. U.S.A.* **2006**, *103*, 10186. (b) Hayashi, H.; Côté, A. P.; Furukawa, H.; O'Keeffe, M.; Yaghi, O. M. *Nat. Mater.* **2007**, *6*, 501. (c) Banerjee, R.; Phan, A.; Wang, B.; Knobler, C.; Furukawa, H.; O'Keeffe, M.; Yaghi, O. M. *Science* **2008**, *319*, 93. (d) Wang, B.; Côté, A. P.; Furukawa, H.; O'Keeffe, M.; Yaghi, O. M. *Nature* **2008**, *453*, 207. (e) Phan, A.; Doonan, C.; Uribe-Romo, F. J.; Knobler, C. B.; O'keeffe, M.; Yaghi, O. M. *Acc. Chem. Res.* **2009**, *43*, 58.

(7) (a) Lewis, D. W.; Ruiz-Salvador, A. R.; Gmez, A.; Coudert, F. X.; Slater, B.; Cheetham, A. K.; Mellot-Draznieks., C. *CrystEngComm* **2009**, *11*, 2272. (b) Tan, J.-C.; Bennett, T. D.; Cheetham, A. K. *Proc. Natl. Acad. Sci. U.S.A.* **2010**, *1107*, 9938. (c) Wu, T.; Bu, X.; Zhang, J.; Feng, P. *Chem. Mater.* **2008**, *20*, 7377. (d) Wu, T.; Bu, X.; Liu, R.; Lin, Z.; Zhang, J.; Feng, P. *Chem.—Eur. J.* **2008**, *14*, 7771. (e) Bux, H.; Liang, F.; Li, Y.;

Cravillon, J.; Wiebcke, M.; Caro, J. *J. Am. Chem. Soc.* **2009**, *131*, 16000. (f) Li, K. H.; Olson, D. H.; Seidel, J.; Emge, T. J.; Gong, H. W.; Zeng, H. P.; Li, J. *J. Am. Chem. Soc.* **2009**, *131*, 10368.

(8) (a) Zhang, J.; Wu, T.; Zhou, C.; Chen, S.; Feng, P.; Bu, X. *Angew. Chem., Int. Ed.* **2009**, *48*, 2542. (b) Wu, T.; Zhang, J.; Zhou, C.; Wang, L.; Bu, X.; Feng, P. *J. Am. Chem. Soc.* **2009**, *131*, 6111. (c) Zheng, S.; Wu, T.; Zhang, J.; Chow, M.; Nieto, R.; Feng, P.; Bu, X. *Angew. Chem., Int. Ed.* **2010**, *49*, 5362.

(9) (a) Feng, P.; Bu, X.; Stucky, G. D. *Angew. Chem., Int. Ed.* **1995**, *34*, 1745. (b) Baerlocher, C.; Meier, W. M.; Olson, D. H. *Atlas of Zeolite Framework Types*; Elsevier: Amsterdam, 2001.

(10) (a) Maeda, K.; Akimoto, J.; Kiyozumi, Y.; Mizukami, F. *Angew. Chem., Int. Ed.* **1995**, *34*, 1199. (b) Carter, V. J.; Wright, P. A.; Gale, J. D.; Morris, R. E.; Sastre, E.; Perez-Pariente, J. *J. Mater. Chem.* **1997**, *7*, 2287. (c) Jhang, P.; Yang, Y.; Lai, Y.; Liu, W.; Wang, S.-L. *Angew. Chem., Int. Ed.* **2009**, *48*, 742.

(11) Synthesis of $Zn_2(BH(mim)_3)_2(obb)\cdot x(solvent)$ (**BIF-20**): A solid mixture of $Zn(NO_3)_2\cdot 6H_2O$ (0.5mmol), $KBH(mim)_3$ (0.05 g, 0.17mmol), and 4,4′-oxybisbenzoic acid (0.25mmol) was dissolved in a mixed 2-amino-1-butanol (1.5 mL)/CH_3CN (0.5 mL)/*N*,*N*′-dimethylformamide (1.5 mL) solution. The sample was placed in a 20 mL vial and heated at 80 °C for 4 days, and then cooled to room temperature. After washes with ethanol and distilled water, the colorless crystals were obtained (yield: 85%). The phase purity was characterized by powder X-ray diffraction. IR (KBr pellet, cm^{-1}): 3130.2 (s), 2466.7 (m), 1610.4 (s), 1417.6 (s), 1234.3 (s), 1112.8 (s), 1006.7 (s), 879.4 (m), 750.3 (s), 663.5 (m), 451.3 (m). Synthesis of $Zn_2(BH(mim)_3)_2(bpdc)\cdot x(solvent)$ (**BIF-21**): $Zn(NO_3)_2\cdot 6H_2O$(0.5mmol), $KBH(mim)_3$ (0.05 g, 0.17mmol) and diphenic acid (0.25 mmol) in a mixed 2-amino-1-butanol (1.5 mL)/CH_3CN(0.5 mL)/DMF (1.5 mL) solution were placed in a 20 mL vial. The sample was heated at 80 °C for 4 days, and then cooled to room-temperature. A mixture of colorless crystals of **BIF-21** and unidentified powder was obtained.

(12) Diffraction data for **BIFs** were collected on a Saturn 70 charge-coupled device diffractometer equipped with confocal-monochromated Mo Kα radiation (λ = 0.71073 Å) at 173K. The CrystalClear program was used for absorption correction. The structures were solved by direct methods and refined on F^2 by full-matrix, least-squares methods using the SHELXL-97 program package. Crystal data for **BIF-20**: $C_{38}H_{38}B_2N_{12}O_5Zn_2$, rhombohedral, $a = b = 27.2749(18)$ Å, $c = 87.561(5)$ Å, $V = 56411(6)$ Å^3, $T = 173$ (2) K, space group *R*-3*c*, $Z = 36$, 93734 reflections measured, 8190 independent reflections (R_{int} = 0.0392). The final R_1 value was 0.0604 ($I > 2\sigma(I)$). The final wR(F^2) value was 0.1939 ($I > 2\sigma(I)$). The goodness of fit on F^2 was 1.091. Crystal data for **BIF-21**: $C_{38}H_{40}B_2N_{12}O_4Zn_2$, tetragonal, $a = b = 18.8569(4)$ Å, $c = 16.0871(7)$ Å, $V = 5720.3(3)$ Å^3, $T = 173(2)$ K, space group *I*-4, $Z = 4$, 6265 reflections measured, 4303 independent reflections (R_{int} = 0.0350). The final R_1 value was 0.0557 ($I > 2\sigma(I)$). The final wR(F^2) value was 0.1499 ($I > 2\sigma(I)$). The goodness of fit on F^2 was 0.859.

(13) (a) Blatov, V. A.; Carlucci, L.; Ciani, G.; Proserpio, D. M. *CrystEngComm* **2004**, *6*, 377. (b) Alexandrov, E. V.; Blatov, V. A.; Kochetkova, A. V.; Proserpio, D. M. *CrystEngComm* **2011**, *13*, 3947. TOPOS was used to identify the net. For a database of nets, see RCSR (http://rcsr.anu.edu.au/).